Chemical Geology
June 2009, Volume 264, Issues 1-4, Pages 197-206
http://dx.doi.org/10.1016/j.chemgeo.2009.03.007

Free gas and gas hydrates from the Sea of Marmara, Turkey: Chemical and structural characterization

Christophe Bourry[a], Bertrand Chazallon[b], Jean Luc Charlou[a, *], Jean Pierre Donval[a], Livio Ruffine[a], Pierre Henry[c], Louis Geli[a], M. Namik Çagatay[d], Sedat İnan[e] and Myriam Moreau[f]

[a] Département Géosciences Marines, IFREMER, centre de Brest, 29280 Plouzané, France
[b] Laboratoire de Physique des Lasers, Atomes et Molécules (PhLAM), Université Lille 1, UMR CNRS 8523, CERLA, 59655 Villeneuve d'Ascq, France
[c] CEREGE, Aix-Marseille Université, CNRS, Collège de France, 13545 Aix en Provence, France
[d] Istanbul Technical University, Maslak, 34469 Istanbul, Turkey
[e] TUBITAK Marmara Research Centre, Institute of Earth and Marine Sciences, Gebze, Turkey
[f] Laboratoire de Spectrochimie Infra-rouge et Raman, Université Lille 1, UMR CNRS 8516, 59655 Villeneuve d'Ascq, France

*: Corresponding author : Jean Luc Charlou, Tel.: +33 298224262; fax: +33 298224570, email address : Jean.Luc.Charlou@ifremer.fr

Abstract:

Gas hydrates and gas bubbles were collected during the MARNAUT cruise (May–June 2007) in the Sea of Marmara along the North Anatolian Fault system, Turkey. Gas hydrates were sampled in the western part of the Sea of Marmara (on the Western High), and three gas-bubble samples were recovered on the Western High, the Central High (center part of the Sea of Marmara) and in the Çinarcik Basin (eastern part of the Sea of Marmara). Methane is the major component of hydrates (66.1%), but heavier gases such as C_2, C_3, and *i*-C_4 are also present in relatively high concentration. The methane contained within gas hydrate is clearly thermogenic as evidenced by a low $C_1/C_2 + C_3$ ratio of 3.3, and carbon and hydrogen isotopic data ($\delta^{13}C_{CH4}$ of − 44.1‰ PDB and δD_{CH4} of − 219‰ SMOW). A similar signature is found for the associated gas bubbles ($C_1/C_2 + C_3$ ratio of 24.4, $\delta^{13}C_{CH4}$ of − 44.4‰ PDB) which have the same composition as natural gas from*K. Marmara-af* field. Gas bubbles from Central High show also a thermogenic origin as evidenced by a $C_1/C_2 + C_3$ ratio of 137, and carbon and hydrogen isotopic data ($\delta^{13}C_{CH4}$ of − 44.4‰ PDB and δD_{CH4} of − 210‰ SMOW), whereas those from the Çinarcik Basin have a primarily microbial origin ($C_1/C_2 + C_3$ ratio of 16,600, $\delta^{13}C_{CH4}$ of − 64.1‰ PDB). UV-Raman spectroscopy reveals structure II for gas hydrates, with CH_4 trapped in the small (5^{12}) and large ($5^{12}6^4$) cages, and with C_2H_6, C_3H_8 and *i*-C_4H_{10} trapped in the large cages. Hydrate composition is in good agreement with equilibrium calculations, which confirm the genetic link between the gas hydrate and gas bubbles at Western High and the *K.Marmara-af* offshore gas field located north of the Western High. We calculate the characteristics of the hydrate stability zone at Western High and in the Çinarcik Basin using the CSM-GEM computer program. The base of the structure II hydrate stability field is at about 100 m depth below the seafloor at the Western High site, whereas in the Çinarcik Basin, *P–T* conditions at the seafloor correspond to the uppermost range for structure I hydrate formation from microbial gas.

Keywords: Sea of Marmara; Gas hydrate; Gas bubbles; Thermogenic gas; Isotopes

1. Introduction

Hydrocarbon gases, mainly methane, originating from the decomposition of organic matter by biochemical and thermal processes are common in marine sediments. Seafloor manifestations of hydrocarbon gas expulsions are observed on continental shelves and slopes worldwide, and are designated as cold seeps (Judd and Hovland, 2007; Juniper and Sibuet, 1987). Cold seeps are often associated with various seabed surface features such as pockmarks, mud volcanoes, mud diapirs (e.g. Dimitrov and Woodside, 2003; Judd and Hovland, 2007; Juniper and Sibuet, 1987; Le Pichon et al., 1990), or with active faults (e.g. Henry et al., 2002; Trehu et al., 1999; Zitter et al., 2008). However, when conditions of low temperature and high pressure coexist in sediments, gas and water can form a gas hydrate, a crystalline compound with a well-defined structure that consists of a cage network of water molecules with hydrocarbon guests trapped inside the cages. P-T conditions required to initiate the hydrate formation and to stabilize its structure are encountered in marine sediments, mainly in deep waters along continental margins and to a lesser extent in polar regions associated with permafrost (Kvenvolden and Lorenson, 2001). Since the first discovery of natural gas hydrates in permafrost (Makogon, 1965) and in oceanic sediments (Yefremova and Zhizhchenko, 1974), new gas hydrate sites are discovered regularly. However, to date, only 26 sites (reviewed by Sloan and Koh, 2008) could be sampled, partly due to their instability at ambient temperature and to the technological difficulties to recover natural solid samples at high depth.

Natural gas hydrates can form different crystalline structures depending on the nature and size of the guest molecules. Two hydrate structures, I and II, have been recognized since about 1952 (Claussen, 1951; Pauling and Marsh, 1952; Von Stackelberg and Müller, 1951), and a third structure, H, has been discovered by Ripmeester et al. (1987). Structure I is the most common conformation **(**Sloan, 1998) and consists in a body-centered cubic structure organized in two small cages (SC) (pentagonal dodecahedral) and six large cages (LC) (tetracaidecahedral) (McMullan and Jeffrey, 1965). The cages of the structure I are just large enough to include small hydrocarbons, methane and ethane, and non-hydrocarbons such as N_2, CO_2 or H_2S. Structure II (sII) consists of sixteen small cages (pentagonal dodecahedral) and eight large cages (hexacaidecahedral) (Mak and McMullan, 1965). Methane and ethane can occur in sII gas hydrate, but the larger cages can be occupied by hydrocarbons such as propane and isobutane. The structure H (termed sH) is formed by encaging large-size hydrocarbon (such as isopentane) molecules in the presence of a small-size hydrocarbon help-gas molecules (generally methane). The unit cell contains three types of cavities, namely, three regular dodecahedral, two irregular dodecahedral and one irregular icosahedral (Ripmeester and Ratcliffe, 1990; Ripmeester et al., 1987).

Submarine gas hydrates are generally considered as a potential energy resource, which could correspond to more than 50% of the world's recoverable reserve of organic carbon (Kvenvolden, 1999). However, they can also be a significant player in the global climate change (Jacobsen, 2001; Kennett et al., 2000), or in geohazards and slope instability (Dillon et al., 2001; Sultan et al., 2004). The structural and compositional data of natural gas hydrates are important for developing technologies to extract this energy resource from the sea floor and to establish their formation/dissociation rates and stability field. Molecular and isotopic composition of the main hydrate-bound gases are plentifully detailed (Milkov, 2005), but only few physical characterizations have been performed on natural samples from the Gulf of Mexico (Davidson et al., 1986; Yousuf et al., 2004), Black Ridge (Uchida et al., 1999), Mallik (Tulk et al., 2000), Northeast Pacific continental margin off Oregon (Gutt et al., 1999), Cascadia Margin (Yousuf et al., 2004), the Okhotsk sea (Takeya et al., 2006), offshore Vancouver Island (Lu et al., 2005), the Congo-Angola basin (Charlou et al., 2004; Chazallon et al., 2007) and the Nigerian margin (Chazallon et al., 2007; Bourry et al., 2007). The present work extends these physical and chemical studies of natural gas hydrates to new specimens recovered from the Sea of Marmara, during the Marnaut cruise (May-June 2007).

One of the purposes of the interdisciplinary MARNAUT cruise (RV *L'Atalante*) was the study of the relationships between active faults, fluid emission and landslides, which also involved *Nautile* submersible explorations. During this cruise, gas hydrates and vent-gas associated with high fluid outflow at active faults were sampled by sediment coring (hydrates) and during submersible dives (vent gas). Relations between gas emissions and active tectonics within the submerged section of the North Anatolian Fault zone in the Sea of Marmara are presented by Geli et al. (2008). One important issue for understanding the relationship between fluids and seismogenic faults is to determine the depth of origin of the fluids and particularly whether fluids originate from relatively shallow syn-tectonic sediments, or from the basement pre-dating the active basin, and could therefore be related to the seismogenic zone. The distribution of cold seeps in the Sea of Marmara and the geological context lead to hypothesize that at least part of the fluids expelled in the western Sea of Marmara originate from Thrace basin hydrocarbon source rocks (Gürgey et al., 2005), whereas the methane in the eastern Sea of Marmara would be of bacterial origin (Zitter et al., 2008). We report the gas composition and the isotopic signature of gas hydrate and gas bubbles, and the molecular structure of the gas hydrate. These results are compared to thermodynamic model predictions, in order to document the origin, formation and stability of gas hydrates in the Sea of Marmara.

2. Geological settings

The Sea of Marmara is an inland sea between the Thrace and Anatolia (Fig. 1), which together with the Çanakkale (Dardanelles) and Istanbul (Bosphorus) straits, connects the Black Sea and Mediterranean Sea. It covers an area of about 11 110 km² consisting of shelves, deep basins, pressure highs, gulfs and bays. The Sea of Marmara is located on the northern branch of the North Anatolian Fault (NAF) which exhibits about 20-25 mm/yr of strike-slip motion, representing most of the motion between the Anatolian and Eurasian plates (Armijo et al., 2002; Imren et al., 2001; McClusky et al., 2000; Meade et al., 2002). The physiography of the Sea of Marmara consists of an up to 45 km wide southern shelf, a 10-20 km wide northern shelf and in between two a series of E-W trending ca 1250 m deep basins (Tekirdağ, Central, Çinarcik basins) that are separated by NNE-SSW trending ridges (Western High, Central High). Cold seeps are often associated with active faults (Henry et al., 2002; Trehu et al., 1999) but although seeps are frequently associated with compression, strike-slip faults such as the North Anatolian Fault are also involved in expulsion of deep fluids (Chamot-Rooke et al., 2005; Orange et al., 1999; Zitter et al., 2006, 2008). An increase of gas bubbles released into the water column was observed in the Gulf of Izmit after the Kocaeli earthquake (1999) (Alpar, 1999; Kuscu et al., 2005) and gas bubbles were observed escaping from black patches while short sediment push cores were recovered during the MARMARASCARPS (2002) cruise (Armijo et al., 2005). The black patches are iron sulfide-rich sediments attributed to anaerobic methane oxidation by sulfate reduction (Sassen et al., 1993). Active seeps were detected along the main fault scarp on the southern side of the Tekirdağ Basin and along additional faults branching from the Central High and Western High strike-slip faults in the Central Basin (Zitter et al., 2008). In active areas, the seafloor exhibits carbonate crust pavements or chimneys, which are common features of cold seep sites and are considered to be by-products of the oxidation of hydrocarbons (Aloisi et al., 2000; Kulm and Suess, 1990; Kulm et al., 1986). Black patches, and brown and white bacterial mats are also regularly associated with active seep areas (Zitter et al., 2008).

3. Sampling and analytical methods

Gas hydrates from the Sea of Marmara were collected from three gravity cores (MNTKS 25, MNTKS 27, MNTKS 33) recovered in the vicinity of the main fault on Western High (Fig. 1). The gas hydrates were porous, had a yellowish tint, and a distinct smell that may be explained by the presence of traces of petroleum condensate in the pores. Natural yellow or yellow-orange gas hydrates, associated with petroleum condensate, have been previously observed at Barkley Canyon (Hester et al., 2007) or in the Gulf of Mexico (Sassen and MacDonald, 1997). Some specimens, up to 10 cm in diameter, were extracted from the upper part of the 7.15-m-long MNTKS 25 core (667 m water depth, 14.5°C), in the lower part of the 7.10-m-long MNTKS 27 (669 m water depth, 14.5°C) core and in the totality of the 10-m-long MNTKS 33 core (658 m water depth, 14.5°C). The recovered pieces were first stored at –80°C in a freezer on board before being quickly shipped to France. The samples were placed in liquid nitrogen at –196°C to avoid further decomposition before laboratory analysis. Natural gas hydrate samples are inexorably associated with relatively large amount of ice. It is suggested that ice forms during the recovery when the hydrates are outside their p-T stability field, or originates from seawater that is generally attached to the gas hydrates and converts to ice when using liquid nitrogen for sample preservation (Bohrmann et al., 2007; Bourry et al., 2007). Free gas naturally venting from the seafloor was collected (PG-1659, PG-1662, PG-1664) (Fig. 1) using the PEGAZ sampler (Charlou et al., 2007), manipulated by the arm of the research submersible *Nautile.* Gas flow displaces ambient seawater in gas-tight high pressure sampling cells within ~1 m of the seafloor. One gas bubbles sample (PG-1662, 666 m water depth) was collected in the vicinity of the gas hydrates collection area on the Western High and this intimate association suggests that the vent gas is representative of the hydrocarbon pool from which the gas hydrate crystallized. Other samples of gas bubbles were collected from active vent on the Central High (PG-1664, 329 m water depth) and cold seeps in the southern Çinarcik Basin (PG-1659, 1248 m water depth) where no gas hydrates were found. The analytical work on the gas hydrate samples was performed onshore both at the laboratory Géochimie-Métallogénie at IFREMER-Brest and at TUBITAK Marmara Research Centre, one month after the cruise. Each cell containing the gas at in-situ pressure was connected to an extraction line permitting gas transfer into glass tubes at an appropriate pressure for gas composition and isotopic analyses. Gas hydrate specimens were also placed in a high pressure sampling cell for gas and isotopes measurements after gas hydrate decomposition.

We used gas chromatography to measure the composition of gas bubbles and of gas issued from the hydrate decomposition. Isotopic measurements are performed at Isolab laboratory (The Netherlands) by gas chromatography–isotope ratio–mass spectrometry (GC-IR-MS). The $\delta^{13}C$ values are reported as parts per thousand (‰) relative to the PeeDee Belemnite standard (PDB), and the δD values are reported as ‰ relative to the standard mean ocean water (SMOW) standard.

The natural gas hydrates are analyzed by Raman spectroscopy using a LabRam HR 800 UV (Jobin-Yvon) equipped with a back-illuminated CCD detector in Lille. The gas hydrates are crushed in liquid nitrogen and loaded into a pre-cooled dedicated LINKAM stage mounted onto a BX 41 Olympus microscope. The temperature in the stage is set to 133 K to avoid the decomposition of the samples. The excitation line at 266 nm is produced by a MBD-266 Laser source (Coherent) which is focused to a spot size of about 1.7 µm using a x15 LMU OFR objective (N.A. 0.38, working distance of 8.5 mm). The laser power at the sample is ~10 mW, thus avoiding sample damage. The acquisition time is set to 300 s/ spectra. The obtained spectra are then baseline corrected and analyzed with a least-square fitting protocol (PeakFit4) using Voigt area profiles. This procedure allows a precise determination of the integrated band intensities collected with a high signal to noise ratio.

4. Results and discussion

4.1. Gas and isotopic composition: origin of gas hydrates and gas bubbles

Gas and isotopic composition data for gas hydrate (MNTKS 27) and gas bubbles (PG-1659, PG-1662 and PG-1664) are reported in Table 1. Composition of gas hydrate samples collected on Western High ranges from 66.1 to 82 % for CH_4 (66.1 % CH_4 in MNTKS 27 sample) and from 18 to 29.5 % for C_2 to C_4 (1.23 % C_2, 18.8 % C_3, 9.5 % *i*-C_4 in MNTKS 27 sample). CO_2 (4%) and traces of heavier hydrocarbons are also present. Carbon and hydrogen isotopic ratios in methane are used to identify the specific origin of methane (Coleman et al., 1995; Schoell, 1988; Whiticar, 1999). Methane in natural gases may be of biogenic origin formed via the processes of carbon dioxide reduction (the more common process in marine sediments) or via acetate fermentation (Coleman et al., 1995; Whiticar, 1999; Whiticar et al., 1986). The methane can also form from thermal degradation of kerogen and oil (thermogenic methane) (Schoell, 1988). Microbial hydrocarbon gases form in shallow sediments below the sulfate-reduction zone and are composed mainly of CH_4 depleted in ^{13}C (isotopically lighter, commonly $\delta^{13}C$ < –55‰ PDB), with traces of C_2 and C_3, and thus have increased C_1/C_2+C_3 ratios (commonly > 10 000) (Claypool and Kvenvolden, 1983). In contrast, thermogenic methane is enriched in ^{13}C compared to biogenic methane, with $\delta^{13}C$ > –55‰ PDB, and thermogenic gases are relatively enriched in C_{2+}, with low C_1/C_2+C_3 ratios (< 1000).

Isotopic and molecular composition of gas within the gas hydrate samples from Western High ($\delta^{13}C$ −44.1 ‰ PDB, C_1/C_2+C_3 ratio of 3.3) are characteristic of a thermogenic origin (Fig. 2a). This indicates that the gas hydrate deposit was formed by gas sourced from petroleum or rocks that contain thermally mature organic matter. Furthermore, the thermal origin of methane is also suggested by the correlation of δD CH_4 (−219‰ SMOW) and $\delta^{13}C$ CH_4 values. Typical values of δD and $\delta^{13}C$ for thermogenic methane range between −100‰ and −300‰ SMOW, and −20‰ and −50‰ PDB respectively (Schoell, 1988). $\delta^{13}C$ and δD values of CH_4 for MNTKS 27 gas hydrates are comparable to $\delta^{13}C$ values ranging from −42.2‰ to −49.9‰ PDB and δD values from −161‰ to −203‰ SMOW, respectively, derived from thermogenic gas hydrates from the Gulf of Mexico (Sassen et al., 2001a; Sassen et al., 2001b). Comparable $\delta^{13}C$ values of methane ranging from −42.6‰ to −43.4‰ PDB and δD values from −138‰ to −143‰ SMOW were also reported for hydrates from the northern Cascadia margin (Canyon Barkley, offshore Vacouver Island; Pohlman et al., 2005), and for hydrates recovered offshore Costa Rica ($\delta^{13}C$ −44‰ PDB, δD −137‰ SMOW; Hensen et al., 2004). Other thermogenic gas hydrates were also recovered from the Middle America Trench during the DSDP Leg 84 ($\delta^{13}C$ −41.9‰ PDB; Kvenvolden and McDonald, 1985) and from the Caspian Sea ($\delta^{13}C$ −44.8‰ PDB; Ginsburg et al., 1992; Ginsburg and Soloviev, 1998).

Gas bubbles PG-1659, collected on the southern part of the Çinarcik Basin, are mainly composed of methane (99.63%) with only trace amounts of CO_2 (0.1%) and heavier hydrocarbons (<0.005%). The plot of hydrocarbon composition versus stable carbon isotope values (Fig. 2a) clearly indicates that methane leaking from the seafloor on the southern part of the Çinarcik Basin has a biogenic signature and confirms hypothesis of Zitter et al. (2008) concerning the biogenic origin of gas in the eastern part of the Sea of Marmara. In addition, the value of −64‰ (PDB) for $\delta^{13}C$-CO_2 strongly indicates that the methane in these gas bubbles is mainly produced by microbial CO_2 reduction, and not via bacterial acetate fermentation (Whiticar, 1999). The ethane, on the other hand, has apparently a thermogenic origin as indicated by its higher $\delta^{13}C$ values (Fig. 2b), suggesting that a small amount of thermogenic gases are mixed with the microbial methane in the Çinarcik Basin. Such mixing of biogenic methane and thermogenic ethane in hydrates was previously observed in various oceanic environments such as the Black Sea (Blinova et al., 2003), Hydrate Ridge (Milkov et

al., 2005), offshore Northern California (Eel River; Brooks et al., 1991), which are all characterized by a high free gas flux.
Gas bubbles of sample PG-1664 (on the Central High) also contain a high amount of CH_4 (98.86%) with C_2, C_3 and CO_2 concentration (0.48%, 0.24% and 0.36% respectively) being relatively higher than those in sample PG-1659 from the southern part of the Çinarcik Basin, indicating that methane from Central High has a thermogenic origin (Fig. 2a and 2b). Finally, PG-1662 bubbles sampled in the vicinity of the gas hydrate area, on the Western High have similar gas and isotopic composition to the gas contained in the gas hydrate. This intimate association suggests that the gas hydrates have crystallized from this associated vent gas. Bubbles from the Western High contain 90.90% CH_4, with relatively large amounts of C_2 (1.23%), C_3 (2.50%), i-C_4 (0.93%), n-C_4 (0.15%), i-C_5 (0.31%) and CO_2 (3.90%). The composition of vent gas from the Western High has high similarity with the *K.Marmara-af* natural gas field located offshore Silivri on northern shelf (Gürgey et al., 2005). These similarities of composition strongly suggest the migration of natural gas from the Thrace Basin underlying part of the Sea of Marmara floor. The distribution of cold seeps in the Sea of Marmara and the geological context lead also to hypothesize that at least part of the fluids expelled in the fault on the Western High and the natural gas of the *K.Marmara-af* natural gas field originate from a similar source rock. At the Western High, $\delta^{13}C$ of methane and heavier hydrocarbons are similar in bubbles and gas hydrates. In addition, the C_1/C_2+C_3 ratio is consistent with a thermogenic origin of the gas (Fig. 3a). Relative to vent gas, methane of gas hydrate occurs in lower percentage (66.1%) and C_3 and i-C_4 are proportionally higher. This difference of composition between hydrate-bound gases and associated vent gas is characteristic of molecular fractionation involved during the gas hydrate formation, and confirms that the preferential enclathration in the hydrate cages is $CH_4 < C_2 < C_3 <$ i-C_4 (Sassen et al., 1999; Sloan, 1998; Uchida et al., 2007). However, significant carbon or hydrogen isotopic fractionation of the hydrocarbons does not occur during gas hydrate crystallization (Brooks et al., 1986; Claypool et al., 1985; Sassen and McDonald, 1997).
The stable carbon isotope composition of C_1-C_5 hydrocarbon gases from Western High and Central High are consistent with a thermogenic origin, whereas the ^{13}C-depleted methane escaping from the Çinarcik Basin suggests a microbial origin. The substantial differences of $\delta^{13}C$-CO_2 observed from hydrate and all gas bubble samples are also interesting. CO_2 of hydrate and gas bubbles from Western High and Central High are enriched in ^{13}C by as much as 38 ‰ relative to bacterial vent gas from the Çinarcik Basin (Table 1), and ranges from +25.6 ‰ to +29.1 ‰ PDB. Such high values, generally up to +15 to +20 ‰ PDB, are consistent with heavily biodegraded oil (Jones et al., 2008; Masterson et al., 2001; Pallaser, 2000). Biodegradation of crude oil in subsurface petroleum reservoirs is dominated by anaerobic hydrocarbon degradation, including methanogenesis (Larter and di Primio, 2005), which is the likeliest fate of most carbon dioxide produced as the terminal oxidation product during biodegradation (Head et al., 2003; Jones et al., 2008). Jones et al. (2008) suggest that methanogenic hydrocarbon degradation occurs predominately via syntrophic oxidation of alkanes to acetate and hydrogen, and the produced carbon dioxide is reduced to methane during hydrogenotrophic methanogenesis. With increasing hydrocarbon conversion, carbon dioxide becomes ^{13}C enriched (Jones et al., 2008). Thus, the isotopically heavy carbon dioxide in vent gas and hydrate from the Sea of Marmara, with $\delta^{13}C$ CO_2 values up to +25.6 ‰, is the signature of heavily degraded oil reservoirs.

4.2. Molecular structure discrimination

As previously carried out on the gas hydrates collected from African and Norwegian margins (Charlou et al., 2004; Chazallon et al., 2007), the samples collected in the Sea of Marmara were first investigated by micro-Raman spectroscopy using the excitation line at 514.5 nm produced by an Ar^+ laser. However, this proved to be unsuccessful due to the high degree of background interference caused by fluorescence effects generated by the inherent presence of sediments at the sample surface. This difficulty has also been encountered by

Hester et al. (2007), who could not analyze the yellowish hydrates from the Barkley Canyon spectroscopically. To solve this analytical problem, the natural samples from the Sea of Marmara are here analyzed using a UV excitation line at 266 nm.

Fig. 3 shows typical Raman spectra of natural gas hydrate recorded at atmospheric pressure and 133 K in the 2800-3800 cm^{-1} spectral range. The spectral region ranging from 2800 to 3000 cm^{-1} (Fig. 3b) corresponds to the C-H bond stretching of hydrocarbons. Two bands can be observed at ~2903 and ~2913 cm^{-1}, corresponding to the C-H bond stretching (ν_1 mode) of methane in the hydrate structure. The integrated intensity ratio of the methane peaks (2903:2913 cm^{-1}) is 0.3, and indicates that this hydrate crystallizes in a type II structure. Indeed, for methane-rich mixtures with hydrate guests which don't fit in the small cages (such as C_2H_6, C_3H_8, i-C_4H_{10}), the intensities ratio of methane in the sII large and small cages should be less than 0.5 (there is twice more small cages than large cages in the type II structure; Sloan, 1998). This is because, in such mixtures, methane will occupy most of the small cages of sII and the larger guests will occupy at least some of the sII large cages, along with methane (Hester et al., 2007). The peak at ~2903 cm^{-1} can thus be assigned to the C-H stretching of CH_4 within the large cages ($5^{12}6^4$) and the peak at ~2913 cm^{-1} to the C-H stretching of CH_4 within the small cages (5^{12}) (Sum et al., 1997). In comparison, only a single band corresponding to ν_1 is observed for methane in free gas at ~2916 cm^{-1} (Chazallon et al., 2007). The splitting of the ν_1 band in hydrate can be attributed to a perturbation of the local electrostatic fields produced by water molecules forming cages of different types (Tulk et al., 2000). The methane in the large cages has a more negative frequency shift, relative to the gas phase, than methane in the small cages (Subramanian and Sloan, 2002). Although Raman spectroscopy proves to be a powerful tool to obtain detailed spectral features characterizing the enclathrated gas components in natural gas hydrates, it doesn't allow to distinguish sII hydrate from sH hydrate. Complementary analyses are necessary in order to dismiss the hypothesis of the presence of sH hydrate in natural samples from the Sea of Marmara. A mixture of type II and type H structures has already been observed for example in natural hydrate sample recovered from Barkley canyon, on the northern Cascadia margin (Lu et al., 2007). Structure II gas hydrate can be oil-related and has been identified from sediments of the Gulf of Mexico (Brooks et al., 1986; Brooks et al., 1984) and from the Caspian Sea (Ginsburg and Soloviev, 1998). Asterisks on the Fig. 3b mark smaller bands attributed to C-H stretching modes of C_2, C_3 and *i*-C_4 (Hester et al., 2007; Uchida et al., 2007). The spectral region at ~3100 cm^{-1} (Fig. 3a) corresponds to the O-H spectral region of water. The weak band at ~3053 cm^{-1} characterizes the presence of hydrates and is assigned to an overtone of the doubly degenerate vibration ν_2 of methane (Chazallon et al., 2007).

The spectral region ranging from 750 to 1050 cm^{-1} corresponds to the C-C stretching of hydrocarbons (Fig. 4a). The bands at ~812 and ~876 cm^{-1} can be respectively assigned to the ν_7 symmetric C-C stretching vibration of *i*-C_4 (Hester et al., 2007; Uchida et al., 2007) and to the ν_8 C-C stretching of C_3 (Hester et al., 2007; Kawamura et al., 2006) in the large $5^{12}6^4$ cavities of sII structure. The unknown peak at ~975 cm^{-1}, which was also reported by Uchida et al. (2007), has not yet been assigned. Lastly the C_2 ν_3 symmetric C-C stretching in the $5^{12}6^4$ cages can be clearly seen at ~992 cm^{-1} (Hester et al., 2007; Uchida et al., 2002), while the corresponding peak for ethane in the large cage of sI hydrate at 1001 cm^{-1} is absent, confirming the presence of a sII dominated hydrate. These results confirm that C_2, C_3, and *i*-C_4 molecules are encaged only into the $5^{12}6^4$ cages of the sII structure. The bands at ~1274 cm^{-1} and ~1380 cm^{-1} on spectral region ranging from 1250 to 1400 cm^{-1} (Fig. 4b) can be assigned to the CO_2 vibration, whereas the band at ~1328 cm^{-1} has not yet been attributed. Comparatively, the characteristic signature of CO_2 in sI natural hydrates from the Congo-Angola Basin was reported by Charlou et al. (2004) with two bands at ~1274 and ~1377 cm^{-1}.

4.3. Chemistry and modeling: origin of the gas forming the hydrate and hydrate stability field

Differing composition of our gas-bubbles samples predict different gas hydrate structures and thus variant gas hydrate stability conditions. We used flash calculation, which is a thermodynamic algorithm using a combination of methods and computational strategy, to describe the behavior of mixtures depending on the p-T seafloor conditions. In general, by changing the p-T conditions for a given mixtures lead to the formation of different phases in equilibrium. Thus, the aim of the flash calculation is, using thermodynamic equations, to identify the phases in equilibrium as well as the distribution of each component in each phase (Michelsen and Mollerup, 2004). Others thermodynamic and thermophysic properties can be determine as well. A first flash calculation shows that depending on the p-T seafloor conditions, the thermogenic gas bubbles of sample PG-1662 (Western High) could give rise to structure II and even structure H hydrate (Sloan and Koh, 2008), whereas the biogenic gas bubbles PG-1659 (Çinarcik Basin) can form only structure I.
Here, flash calculations have been performed on gas bubbles mixing with pore water in order to evaluate whether they will lead to gas hydrate and what will be the composition of both the hydrate and the remaining gas bubbles. The Raman signature of the associated gas hydrate suggests the presence of structure II, and is thus consistent with formation from the gas bubbles (sample PG-1662).
The locations of ours samples (except PG-1659) are within a region underlain by southern extension of the Thrace Basin, a well-known natural gas-producing province in Turkey (Gürgey et al., 2005). The sampled gas bubbles may migrate from one of the Thrace Basin gas fields or originate from similar source rock. During migration, this gas could form gas hydrate under appropriate T and P conditions within the sediments.
Here, we compare measured gas composition to results obtained by thermodynamics modeling in order to get insight into the origin and stability of the hydrate associated with the bubbles of sample PG-1662, and also to understand the absence of hydrate for PG-1659. The CSM-GEM computer hydrate program (Sloan and Koh, 2008) has been used for the modelling. This program incorporates the Van der Waals and Platteeuw model (Van der Waals and Platteeuw, 1959) along with performing a Gibb's energy minimization to evaluate the stable phases in equilibrium and determine their composition. Because the program performs constant volume flash calculations, the approach proposed by Hester et al. (2007) has been followed. Thus, each flash calculation is based on the conversion of 1 mol of liquid water to hydrate, in contact with 100 mol of natural gas.

4.3.1. Hypothesis on the origin of the PG-1662 gas bubbles

The *K.Marmara-af* natural gas field reservoir or similar source rock are likely the source of bubbling gases at PG-1662 sampling site because of similar gas compositions. Two questions arise: 1) will this natural gas source form gas hydrate under the P-T conditions at the sampling site?, and 2) is the composition of the sampled gas hydrate consistent with theoretical predictions based on gas source and gas fractionation as gas hydrate forms? Flash calculations have been done for both the *K.Marmara-af* natural gas and the sampled gas bubbles. Based on the seafloor conditions, the flash was calculated at 6.69 MPa and 14.5°C for both gas compositions. The calculated hydrate composition using PG-1662 gas bubbles composition is presented in Table 2 ($X_{i,hyd,calc}$) and compared to the measured data obtained by gas chromatography for natural gas hydrate from Western High ($X_{i,exp}$). The calculated hydrate composition is similar to the analyzed one and confirm that gas hydrate has crystallized from the associated vent gas (PG-1662 gas bubbles sample). Moreover, the composition of the *K.Marmara-af* gas field is very close to the sampled gas bubbles. For both systems, the flash calculation successfully predicted structure II gas hydrate as the more stable structure under the seafloor conditions. This is in agreement with the Raman spectroscopic results obtained on the sampled gas hydrate. The calculated hydrate composition is also similar to the analyzed one, strengthening our hypothesis that gas from

the *K.Marmara-af* field or from the same source rock migrate to the Western High. The flash calculations done for the *K.Marmara-af* natural gas and the sampled gas bubbles PG-1662 also confirm that the preferential enclathration in the hydrate cages is $CH_4 < C_2 < C_3 < i\text{-}C_{4+}$.

4.3.2. Hydrate stability zone of the gas bubbles from PG-1659 and PG-1662

The depth of the water column over the investigated area of the Sea of Marmara is highly variable , and the gas bubbles sampled are also very different in composition (Table 1). The CSM-GEM computer hydrate program has been used to describe the hydrate stability zone where we collected PG-1662 gas bubbles sample, and also where PG-1659 gas bubbles have been sampled because no gas hydrates are found in these sediments although there is an ample source of methane. Hydrate formation and stability is function of P-T conditions, gas composition, gas concentration in sediments which must be sufficient, and the pore water salinity, which is about 38 PSU (unpublished data) for our area of investigation. Measurements of the thermal gradient of the sediments have been done for this area during the same MARNAUT cruise (Andre, 2008).
In the case of sample PG-1662 site, where gas hydrate is found, the temperature at the seafloor is 14.5°C with a pressure of 6.69 MPa. Structure II gas hydrates are stable at these temperature and pressure conditions, as confirmed by our gas hydrate samples. Moreover, our calculations estimate the thickness of the gas hydrate stability zone to be ca. 100 m with the base of the zone at 19°C and 7.84 MPa (Fig. 5a).
Concerning the PG-1659 area, where the biogenic gas bubbles can only form structure I hydrate, gas hydrate may not be able to form in detectable amounts at the seafloor, as conditions (14°C and 12 Mpa) correspond to the limit conditions for gas hydrate formation. In principle, gas hydrate could be stable in the first meters of sediments (Fig. 5b), but no gas hydrate associated with the PG-1659 gas bubbles were recovered at 1200 m water depth in the Çınarcık Basin. This may be explained because kinetics of hydrate formation will be very slow under these conditions and the hydrates eventually formed will be sensitive to small variations of pressure and temperature. Important variations generally occur during the recovery process and may result in a complete dissociation of the hydrate, especially if gas hydrates are microscopic.

5. Conclusions

In this paper we document the chemical and physical characteristics of the natural gas hydrate occurring on the active North Anatolian Fault in the Sea of Marmara. The gas hydrate were collected in the first meters of sediment, along the main fault on Western High, and gas bubbles naturally venting from the seafloor were collected at three sites: Western High, Central High and the southern part of the Çinarcik Basin.

Gas hydrate specimens contain mainly methane, with relatively high amounts of ethane, propane and iso-butane. Carbon and hydrogen isotopes from these collected gases, as well as the C_1/C_2+C_3, ratio attest a thermogenic origin. The composition of gas bubbles emanating from the gas hydrate locality is consistent with that of gas hydrates. The gas bubbles contain thermogenic methane and are likely sourced from the natural gas reservoirs of the Thrace Basin, or from their source rocks. Gas bubbles from Central High also show a thermogenic origin whereas gas bubbles sampled on the Çinarcik Basin are composed of biogenic methane, mixed with a trace amount of thermogenic ethane.

Gas hydrate specimens have been analyzed by UV-Raman spectroscopy. The two bands observed at ~2903 and ~2913 cm^{-1}, characteristic of methane vibration, and the integrated ratio of these peaks (2903:2913 cm^{-1}) being 0.3 show that hydrate crystallizes in a type II structure. C_2, C_3, *i*-C_4 and CO_2 are found to be co-clathrated with methane and confirm the type II structure.

Results obtained from modeling using the CSM-GEM computer hydrate program confirm the type II structure, in agreement with Raman spectroscopy data. In addition, the comparison between measured data and modeling results corroborates our hypothesis on the existence of a link between the gas hydrates, the gas bubbles on Western High and the source rock of the *K.Marmara-af* natural gas field of the Thrace Basin. At Western High, the estimated thickness of hydrate stability zone is about one hundred meters, whereas P-T conditions in the Çinarcik Basin correspond to the uppermost range for gas hydrate formation from microbial gas, but no gas hydrates were collected in this area during MARNAUT cruise.

Acknowledgements

Shiptime, logistics and operations of the MARNAUT cruise (2007) were supported by IFREMER, INSU, ANR (through CATELL-ISIS project), ITU (Istanbul Technical University) and MTA (Maden Tetkik ve Arama, Ankara). We kindly thank captains, officers and crew on-board of the RV *Atalante* and the *Nautile* staff who permitted the recovery of gas bubbles and gas hydrates. We are grateful to L. Bignon who devoted his undivided attention to the sampling of gas bubbles using the new PEGAZ sampler and to the storage of gas hydrates in good conditions for laboratory analysis on shore. We are also grateful for constructive reviews of the manuscript by W. S. Borowski, and an anonymous reviewer.

References

Aloisi, G., Pierre, C., Rouchy, J.-M., Foucher, J.P., Woodside, J., 2000. Methane-related authigenic carbonates of eastern Mediterranean Sea Mud Volcanoes and their possible relation to gas hydrate destabilisation. Earth and Planetary Science Letters 184, 321-338.

Alpar, B., 1999. Underwater signatures of the Kocaeli earthquake of 17 August 1999 in Turkey. Turkish Journal of Marine Sciences 5 111–130.

Andre, C., 2008. Analysis of heat flux data collected during MARNAUT campaign. Internal communication, IFREMER.

Armijo, R., Meyer, B., Navarro, S, King, G., 2002. Symetric slip partitioning in the Sea of Marmara pull-apart: a clue to propagation processes of the North Anatolian Fault? Terra Nova 13 80-86.

Armijo, R., Pondard, N., Meyer, B., Ucarkus, G., de Lepinay, B.M., Malavieille, J., Dominguez, S., Gustcher, M.A., Schmidt, S., Beck, C., Cagatay, N., Cakir, Z., Imren, C., Eris, K., Natalin, B., Ozalaybey, S., Tolun, L., Lefevre, I., Seeber, L., Gasperini, L., Rangin, C., Emre, O., Sarikavak, K., 2005. Submarine fault scarps in the Sea of Marmara pull-apart (North Anatolian Fault): Implications for seismic hazard in Istanbul. Geochemistry Geophysics Geosystems 6, Q06009.

Blinova, V.N., Ivanov, M.K., Bohrmann, G., 2003. Hydrocarbon gases in deposits from mud volcanoes in the Sorokin Trough, north-eastern Black Sea. Geo-Marine Letters 23, 250-257.

Bohrmann, G., Kuhs, W. F., Klapp, S. A., Techmer, K. S., Klein, H., Murshed, M. M., Abegg, F., 2007. Appearance and preservation of natural gas hydrate from Hydrate Ridge samples during ODP Leg 204 drilling. Marine Geology 244, 1-14.

Bourry, C., Charlou, J.L., Donval, J.P., Brunelli, M., Focsa, C., Chazallon, B., 2007. X-ray synchrotron diffraction study of natural gas hydrates from African margin. Geophysical Research Letters 34, L22303.

Brooks, J.M., Cox, H.B., Bryant, W.R., Kennicutt II, M.C., Mann, R.G., McDonald, T.J., 1986. Association of gas hydrates and oil seepage in the Gulf of Mexico. Organic Geochemistry 10, 221-234.

Brooks, J.M., Field, M.E., Kennicutt, M.C., 1991. Observations of gas hydrates in marine-sediments, offshore northern California. Marine Geology 96, 103-109.

Brooks, J.M., Kennicutt, M.C., Fay, R.R., Mcdonald, T.J., Sassen, R., 1984. Thermogenic gas hydrates in the Gulf of Mexico. Science 225, 409-411.

Chamot-Rooke, N., Rabaute, A., Kreemer, C., 2005. Western Mediterranean ridge mud belt correlates with active shear strain at the prism-backstop geological contact. Geology 33, 861-864.

Charlou, J.L., Donval, J.P., Bourry, C., Chaduteau, C., Lanteri, N., Bignon, L., Foucher, J.P., Nouzé, H., the Vicking Scientific team, 2007. Gas bubbles and gas hydrates sampling from Hakon Mosby Mud Volcano - Preliminary results - VICKING cruise (2006), European Geosciences Union, General Assembly, Vienna.

Charlou, J.L., Donval, J.P., Fouquet, Y., Ondreas, H., Knoery, J., Cochonat, P., Levache, D., Poirier, Y., Jean-Baptiste, P., Fourre, E., Chazallon, B., ZAIROV Leg 2 Sci Party, 2004. Physical and chemical characterization of gas hydrates and associated methane plumes in the Congo-Angola Basin. Chemical Geology 205, 405-425.

Chazallon, B., Focsa, C., Charlou, J.-L., Bourry, C., Donval, J.-P., 2007. A comparative Raman spectroscopic study of natural gas hydrates collected at different geological sites. Chemical Geology 244, 175-185.

Clausen, W.F., 1951. A second water structure for inert gas hydrates. Journal of Chemical Physics 19, 1425-1426.

Claypool, G.E., Kvenvolden, K., 1983. Methane and other Hydrocarbon Gases in Marine Sediment. Annual Review of Earth and Planetary Sciences 11, 299-327.
Claypool, G.W., Threlkeld, C.N., Mankewicz, P.N., Arthur, M.A., Anderson, T.A., 1985. Isotopic composition of interstitial fuids and origin of methane in slope sediment of the Middle America Trench, Deep Sea Drilling Project Leg 84. In: R. von Heune, J. Aubouin, et al. (Ed.), Initial Reports, Deep Sea Drilling Project 84. Government Printing Office, Washington, DC, pp. 683-691.
Coleman, D.D., Chao-Li, L., Hackley, K.C., Pelphrey, S.R., 1995. Isotopic identification of landfill methane. Environmental Geosciences 2, 95- 103.
Davidson, D.W., Garg, S.K., Gough, S.R., Handa, Y.P., Ratcliffe, C.I., Ripmeester, J.A., Tse, J.S., 1986. Laboratory analysis of a naturally occurring gas hydrate from sediment of the Gulf of Mexico. Geochimica et Cosmochimica Acta 50, 619.
Dillon, W.P., Nealon, J.W., Taylor, M.H., Lee, M.W., Drury, R.M., Anton, C.H., 2001. Seafloor collapse and methane venting associated with gas hydrate on the Blake Ridge - Causes and implications to seafloor stability and methane release. In: C.K. Paull and W.P. Dillon (Ed.), Natural Gas Hydrates: Occurrence, Distribution, and Detection, Geophysical Monograph Series. AGU, Washington D.C., pp. 211-233.
Dimitrov, L. and Woodside, J., 2003. Deep Sea pockmark environments in the Eastern Mediterranean. Marine Geology, 195, 263-276.
Ginsburg, G.D., Guseynov, R.A., Dadashev, A.A., Ivanova, G.A., Kazantsev, S.A., Soloviev, V.A., Telepnev, E.V., Askeri-Nasirov, P.Y., Yesikov, A.A., Mal'tseva, V.I., Mashirov, G.Y., Shabayeva, I.Y., 1992. Gas hydrates of the southern Caspian. International Geology Review 43, 765-782.
Ginsburg, G.D., Soloviev, V.A., 1998. Submarine gas hydrates. VNII Okeangeologia,, St. Petersburg (Ru), 216 pp.
Gürgey, K., Philip, R.P., Clayton, C., Emiroglu, H., Siyako, M., 2005. Geochemical and isotopic approach tomaturity / source / mixing estimation for natural gas and associated condensates in the Thrace Basin, NW Turkey. Applied Geochemistry 20, 2017-2037.
Gutt, C., Asmussen, B., Press, W., Merkl, C., Casalta, H., Greinert, J., Bohrmann, G., Tse, J.S., Hüller, A., 1999. Quantum rotations in natural methane-clathrates from the Pacific sea-floor. Europhysics Letters 48, 269.
Head, I.M., Jones, D.M., Larter, S.R., 2003. Biological activity in the deep subsurface and the origin of heavy oil. Nature 426, 344-352.
Henry, P., Lallemant, S., Nakamura, K., Tsunogai, U., Mazzotti, S., Kobayashi, K., 2002. Surface expression of fluid venting at the toe of the Nankai Wedge and implications for flow paths. Marine Geology 187, 119-143.
Hensen, C., Wallmann, K., Schmidt, M., Ranero, C.R., Suess, E., 2004. Fluid expulsion related to mud extrusion off Costa Rica - A window to the subducting slab. Geology 32, 201-204.
Hester, K.C., Dunk, R.M., Walz, P.M., Peltzer, E.T., Sloan, E.D., Brewer, P.G., 2007. Direct measurements of multi-component hydrates on the seafloor: Pathways to growth. Fluid Phase Equilibria 261, 396-406.
Imren, C., Le Pichon, X., Rangin, C., Demirbag, E., Ecevitoglu, B., Gorur, N., 2001. The North Anatolian Fault within the Sea of Marmara: a new interpretation based on multi-channel seismic and multi-beam bathymetry data. Earth and Planetary Science Letters 186, 143-158.
Jacobsen, S.B., 2001. Earth science - Gas hydrates and deglaciations. Nature 412, 691-693.
Jones, D.M., Head, I.M., Gray, N.D., Adams, J.J., Rowan, A.K., Aitken, C.M., Bennett, B., Huang, H., Brown, A., Bowler, B.F.J., Oldenburg, T., Erdmann, M.,

Larter, S.R., 2008. Crude-oil biodegradation via methanogenesis in subsurface petroleum reservoirs. Nature 451, 176-181.
Judd, A., Hovland, M., 2007. Seabed Fluid Flow, the impact on geology, biology and the marine environment. Cambridge University Press, New York, 475 pp.
Juniper, S.K., Sibuet, M., 1987. Cold seep Benthic communities in Japan subduction zones-spatial-organization, trophic strategies and evidence for temporal evolution. Marine Ecology-Progress Series 40, 115-126.
Kawamura, T., Sakamoto, Y., Ohtake, M., Yamamoto, Y., Komai, T., Haneda, H., Yoon, J.H., Ohga, K., 2006. Dissociation behavior of pellet shaped mixed gas hydrate samples that contain propane as a guest. Energy Conversion and Management 47, 2491-2498.
Kennett, J.P., Cannariato, K.G., Hendy, I.L., Behl, R.J., 2000. Carbon isotopic evidence for methane hydrate instability during quaternary interstadials. Science 288, 128-133.
Kulm, L.D., Suess, E., 1990. Relationship between carbonate deposits and fluid venting - Oregon accretionary prism. Journal of Geophysical Research-Solid Earth and Planets 95, 8899-8915.
Kulm, L.D., Suess, E., Moore, J.C., Carson, B., Lewis, B.T., Ritger, S.D., Kadko, D.C., Thornburg, T.M., Embley, R.W., Rugh, W.D., Massoth, G.J., Langseth, M.G., Cochrane, G.R., Scamman, R.L., 1986. Oregon subduction zone-venting, fauna, and carbonates. Science 231, 561-566.
Kuscu, I., Okamura, M., Matsuoka, H., Gokasan, E., Awata, Y., Tur, H., Simsek, M., 2005. Seafloor gas seeps and sediment failures triggered by the August 17, 1999 earthquake in the eastern part of the Gulf of Izmit, Sea of Marmara, NW, Turkey. Marine Geology 215, 193–214.
Kvenvolden, K.A., 1999. Potential effects of gas hydrate on human welfare. Proceedings of the National Academy of Sciences of the United States of America 96, 3420-3426.
Kvenvolden, K., Lorenson, T.D., 2001. The global occurence of natural gas hydrates. In: C.K. Paull and W.P. Dillion (Ed.), Natural gas hydrates: Occurence, Distribution and Detection. Geophysical Monograph. AGU, Washington, pp. 3-18.
Kvenvolden, K.A., McDonald, T.J., 1985. Gas hydrates in the Middle America Trench, Deep Sea Drilling Project Leg 84. In: R. Von Huene, J. Aubouin and al. (Ed.), Initial Reports of the Deep Sea Drilling Project 84. U.S Government Printing Office, pp. 667-682.
Le Pichon, X., Foucher, J.-P., Boulègue, J., Henry, P., Lallemant, S., Benedetti, M., Avedik, F., Mariotti, A., 1990. Mud volcano field seaward of the Barbados accretionary complex: A submersible survey. Journal of Geophysical Research 95, 8931–8943.
Larter, S., di Primio, R., 2005. Effects of biodegradation on oil and gas field PVT properties and the origin of oil rimmed gas accumulations. Organic Geochemistry 36, 299-310.
Lu, H., Seo, Y., Lee, J., Moudrakovski, I., Ripmeester, J.A., Chapman, N.R., Coffin, R.B., Gardner, G., Pohlman, J., 2007. Complex gas hydrate from the Cascadia margin. Nature 445, 303-306.
Lu, H., Moudrakovski, I., Riedel, M., Spence, G., Dutrisac, R., Ripmeester, J., Wright, F., Dallimore, S. 2005. Occcurrence and structural characterization of gas hydrates associated with a cold vent field, offshore Vancouver Island. Journal of Geophysical Research 110, B10204.

Mak, T.W., McMullan, R.K., 1965. Polyhedral clathrate hydrates: X. Structure of the double hydrate of tetrahydrofuran and hydrogen sulfide. Journal of Chemical Physics 42, 2732-2737.
Makogon, Y.F., 1965. A gas hydrate formation in the gas saturated layers under low temperature. Gas Industry 5, 14-15.
Masterson, W.D., Dzou, L.I.P., Holba, A.G., Fincannon, A.L., Ellis, L., 2001. Evidence for biodegradation and evaporative fractionation in West Sak, Kuparuk and Prudhoe Bay field areas, North Slope, Alaska. Organic Geochemistry 32, 411–441.
McClusky, S., Balassanian, S., Barka, A., Demir, C., Ergintav, S., Georgiev, I., Gurkan, O., Hamburger, M., Hurst, K., Kahle, H., Kastens, K., Kekelidze, G., King, R., Kotzev, V., Lenk, O., Mahmoud, S., Mishin, A., Nadariya, M., Ouzounis, A., Paradissis, D., Peter, Y., Prilepin, M., Reilinger, R., Sanli, I., Seeger, H., Tealeb, A., Toksoz, M.N., Veis, G., 2000. Global Positioning System constraints on plate kinematics and dynamics in the eastern Mediterranean and Caucasus. Journal of Geophysical Research - Solid Earth 105, 5695-5719.
McMullan, R.K., Jeffrey, G.A., 1965. Polyhedral clathrate hydrates. IX. Structure of Ethylene Oxide Hydrate. Journal of Chemical Physics 42, 2725-2732.
Meade, B.J., Hager, B.H., McClusky, S.C., Reilinger, R.E., Ergintav, S., Lenk, O., Barka, A., Ozener, H., 2002. Estimates of seismic potential in the Sea of Marmara region from block models of secular deformation constrained by global positioning system measurements. Bulletin of the Seismological Society of America 92, 208-215.
Michelsen, M. L., Mollerup, J. M., 2004. Thermodynamic Models, Fundamentals and Computational Aspects, Tie-Line Publication, Denmark.
Milkov, A.V., 2005. Molecular and stable isotope compositions of natural gas hydrates: A revised global dataset and basic interpretations in the context of geological settings. Organic Geochemistry 36, 681-702.
Milkov, A.V., Claypool, G.E., Lee, Y.J., Sassen, R., 2005. Gas hydrate systems at Hydrate Ridge offshore Oregon inferred from molecular and isotopic properties of hydrate-bound and void gases. Geochimica et Cosmochimica Acta 69, 1007-1026.
Orange, D.L., Greene, H.G., Reed, D., Martin, J.B., McHugh, C.M., Ryan, W.B.F., Maher, N., Stakes, D., Barry, J., 1999. Widespread fluid expulsion on a translational continental margin: Mud Volcanoes, Fault Zones, Headless Canyons, and Organic-Rich Substrate in Monterey Bay, California. Geological Society of America Bulletin 111, 992-1009.
Pallaser, R.J., 2000. Recognising biodegradation in gas/oil accumulations through the $\delta^{13}C$ composition of gas components. Organic Geochemistry 31, 1363–1373.
Pauling, L. and Marsh, R.E., 1952. The structure of chlorine hydrate. Proceedings of the National Academy of Sciences of the United States of America, 38, 112-118.
Pohlman, J.W., Canuel, E.A., Chapman, N.R., Spence, G.D., Whiticar, M.J., Coffin, R.B., 2005. The origin of thermogenic gas hydrates on the northern Cascadia Margin as inferred from isotopic (C-13/C-12 and D/H) and molecular composition of hydrate and vent gas. Organic Geochemistry 36, 703-716.
Rangin, C., Demirbag, E., Imren, C., Crusson, A., Normand, A., Le Drezen, E. and Le Bot, A., 2000. Marine atlas of the Sea of Marmara (Turkey). IFREMER, Brest.
Ripmeester, J.A., Ratcliffe, C.I., 1990. Xenon-129 NMR studies of clathrate hydrates: new guests for structure II and structure H. Journal of Physical Chemistry 94, 8773-8776.
Ripmeester, J.A., Tse, J.S., Ratcliffe, C.I., Powell, B.M., 1987. A new clathrate hydrate structure. Nature, 325, 135-136.

Sassen, R., Joye, S., Sweet, S.T., DeFreitas, D.A., Milkov, A.V., MacDonald, I.R., 1999. Thermogenic gas hydrates and hydrocarbon gases in complex chemosynthetic communities, Gulf of Mexico continental slope. Organic Geochemistry 30, 485-497.
Sassen, R., Losh, S.L., Cathles, L., Roberts, H.H., Whelan, J.K., Milkov, A.V., Sweet, S.T., DeFreitas, D.A., 2001a. Massive vein-filling gas hydrate: relation to ongoing gas migration from the deep subsurface in the Gulf of Mexico. Marine and Petroleum Geology 18, 551-560.
Sassen, R., MacDonald, I.R., 1997. Hydrocarbons of experimental and natural gas hydrates, Gulf of Mexico continental slope. Organic Geochemistry 26, 289-293.
Sassen, R., Roberts, H.H., Aharon, P., Larkin, J., Chinn, E.W., Carney, R., 1993. Chemosynthetic bacterial mats at cold hydrocarbon seeps, Gulf of Mexico continental-slope. Organic Geochemistry 20, 77-89.
Sassen, R., Sweet, S.T., Milkov, A.V., DeFreitas, D.A., Kennicutt, M.C., 2001b. Thermogenic vent gas and gas hydrate in the Gulf of Mexico slope: Is gas hydrate decomposition significant? Geology 29, 107-110.
Schoell, M., 1988. Multiple origins of methane in the earth. Chemical Geology 71, 1-10.
Sloan, E.D., 1998. Clathrate Hydrates of Natural Gases, Second Edition, Revised and Expanded. Marcel Dekker, New York.
Sloan, E.D., Koh, C.A., 2008. Clathrate Hydrates of Natural Gases, Third Edition. Chemical Industries 119. CRC Press, Boca Raton.
Subramanian, S., Sloan, E.D., 2002. Trends in vibrational frequencies of guests trapped in clathrate hydrate cages. Journal of Physical Chemistry B, 106, 4348-4355.
Sultan, N., Foucher, J.P., Cochonat, P., Tonnerre, T., Bourillet, J.F., Ondreas, H., Cauquil, E., Grauls, D., 2004. Dynamics of gas hydrate: case of the Congo continental slope. Marine Geology 206, 1-18.
Sum, A.K., Burruss, R.C., Sloan, E.D., 1997. Measurement of clathrate hydrates via Raman spectroscopy. Journal of Physical Chemistry B 101, 7371-7377.
Takeya, S., Kida, M., Minami, H., Sakagami, H., Hachikubo, A., Takahashi, N., Shoji, H., Soloviev, V., Wallmann, K., Biebow, N., Obzhirov, A., Salomatin, A., Poort, J., 2006. Structure and thermal expansion of natural gas clathrate hydrates. Chemical Engineering Science 61, 2670.
Trehu, A.M., Torres, M.E., Moore, G.F., Suess, E., Bohrmann, G., 1999. Temporal and spatial evolution of a gas hydrate-bearing accretionary ridge on the Oregon continental margin. Geology 27, 939-942.
Tulk, C.A., Ripmeester, J.A., Klug, D.D., 2000. The application of Raman spectroscopy to the study of gas hydrates. Annals of the New York Academy of Sciences 912, 859-872.
Uchida, T., Hirano, T., Ebinuma, T., Narita, H., Gohara, K., Mae, S., Matsumoto, R., 1999. Raman spectroscopic determination of hydration number of methane hydrates. Environmental and Energy Engineering 45, 12.
Uchida, T., Takeya, S., Kamata, Y., Ikeda, I.Y., Nagao, J., Ebinuma, T., Narita, H., Zatsepina, O., Buffett, B.A., 2002. Spectroscopic observations and thermodynamic calculations on clathrate hydrates of mixed gas containing methane and ethane: Determination of structure, composition and cage occupancy. Journal of Physical Chemistry B 106, 12426-12431.
Uchida, T., Takeya, S., Kamata, Y., Ohmura, R., Narita, H., 2007. Spectroscopic measurements on binary, ternary, and quaternary mixed-gas molecules in clathrate structures. Industrial & Engineering Chemistry Research 46, 5080-5087.
Van der Waals, J.H., Platteeuw, J.C., 1959. Clathrate Solutions. Advances in Chemical Physics 2, 1.

Von Stackelberg, M., Muller, H.R., 1951. On the structure of gas hydrates. The Journal of Chemical Physics 19, 1319-1320.
Whiticar, M.J., 1999. Carbon and hydrogen isotope systematics of bacterial formation and oxidation of methane. Chemical Geology 161, 291-314.
Whiticar, M.J., Faber, E., Schoell, M., 1986. Biogenic methane formation in marine and fresh-water environments - CO_2 reduction vs acetate fermentation isotope evidence. Geochimica et Cosmochimica Acta 50, 693-709.
Yefremova, A.G., Zhizhchenko, B.P., 1974. Occurence of crystal hydrates of gas in sediments of modern marine basins. Doklady Akad Nauk SSSR 214, 1179-1181.
Yousuf, M., Qadri, S.B., Knies, D.L., Grabowski, K.S., Coffin, R.B., Pohlman, J.W., 2004. Novel results on structural investigations of natural minerals of clathrate hydrates. Applied Physics A 78, 925.
Zitter, T.A.C., Henry, P., Aloisi, G., Delaygue, G., Çagatay, M.N., Mercier de Lepinay, B., Al-Samir, M., Fornacciari, F., Tesmer, M., Pekdeger, A., Wallmann, K., Lericolais, G., 2008. Cold seeps along the main Marmara Fault in the Sea of Marmara (Turkey). Deep Sea Research Part I: Oceanographic Research Papers 55, 552-570.
Zitter, T.A.C., Huguen, C., ten Veen, J., Woodside, J.M., 2006. Tectonic control on Mud Volcanism in the Anaximander Mountains. In: Y. Dilek and S. Pavlides (Ed.), Post Collisional Tectonics and Magmatism in the Eastern Mediterranean Region. Geological Society of America, Special Paper, pp. 615-631.

Figures

Figure 1

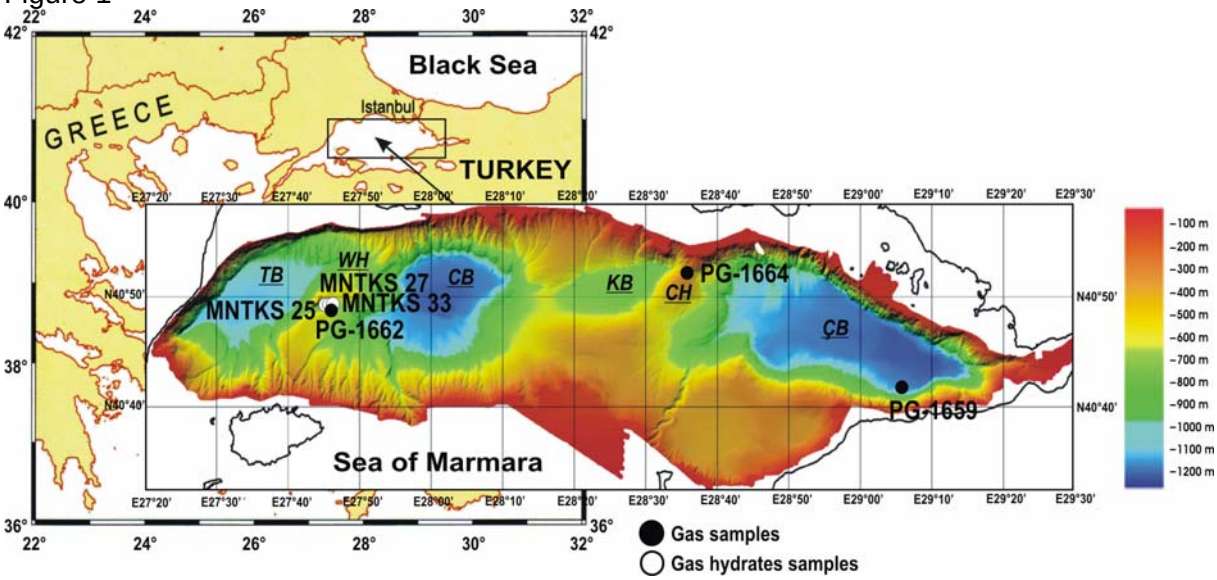

Fig. 1. Bathymetric map of the Sea of Marmara showing the sampling locations of gas hydrates and gas bubbles. Abbreviations: TB, Tekirdağ Basin; CB, Central Basin; KB, Kumbergaz Basin; ÇB, Çinarcik Basin; WH, Western High; CH, Central High (after Rangin et al.; 2000).

Figure 2

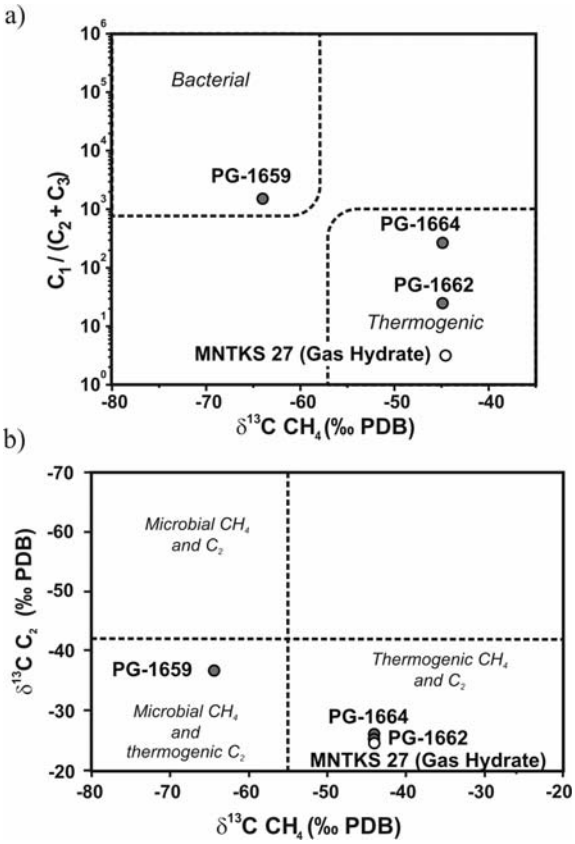

Fig. 2. Determination of the origin of hydrate-bound and bubble gases. a) Relationship between the stable carbon isotope composition ($\delta^{13}C$) of CH_4 and $C_1/(C_2 + C_3)$ ratio (modified from Whiticar, 1999). Bacterial CH_4, as found in the bubbles PG-1659 is characterized by depletion in ^{13}C and a high $C_1/(C_2 + C_3)$ ratio compared to thermogenic CH_4 (bubbles PG-1662, PG-1664 and gas hydrate MNTKS 27). b) Relationship between the stable carbon isotope composition ($\delta^{13}C$) of CH_4 and C_2 in bubbles and hydrate-bound gases (modified from Milkov, 2005). Bubbles PG-1659 contain bacterial CH_4, but C_2 has a thermogenic origin, compared to bubbles PG-1662, PG-1664 and gas hydrate MNTKS 27, which contain both thermogenic CH_4 and C_2.

Figure 3

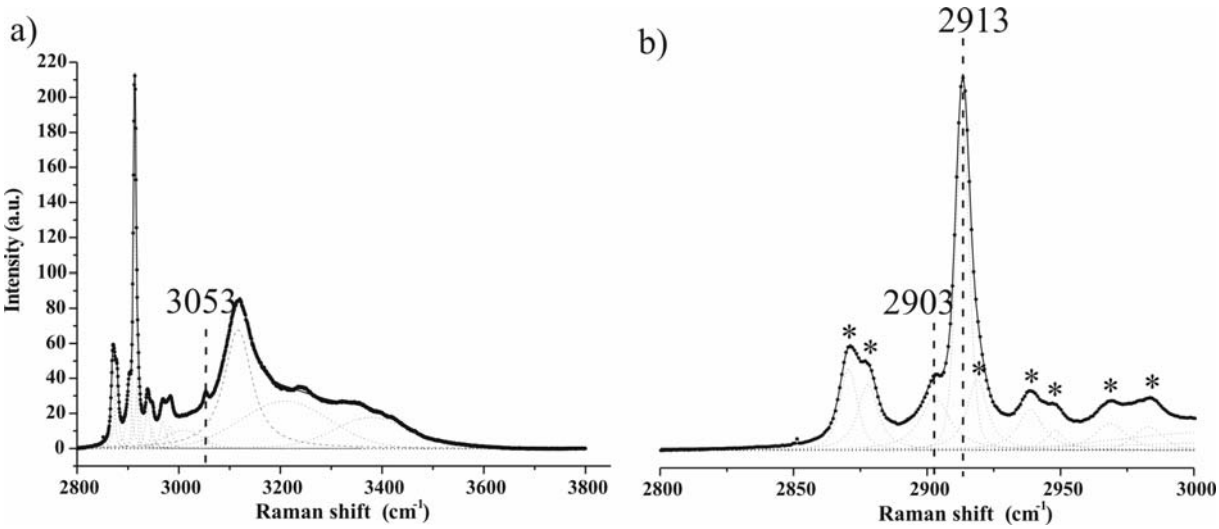

Fig. 3. Typical Raman spectra of natural gas hydrate recorded at atmospheric pressure and 133 K. Connected points correspond to the raw spectrum data. Dotted lines represent the deconvoluted Raman peaks by fitting with a Voigt model. a) C-H stretching spectral regions of hydrocarbons is observed between 2800 and 3000 cm^{-1}. The spectral region at ~3100 cm^{-1} corresponds to the O-H spectral region of water. The weak band at ~3053 cm^{-1} characterizes the presence of hydrates and is assigned to an overtone of methane. b) Enlarged view of the C-H stretching spectral regions of hydrocarbons. The twin bands at ~2903 and ~2913 cm^{-1} are attributed to CH_4 trapped in the large cages ($5^{12}6^4$) and small cages (5^{12}) of the type II structure. Asterisks marked the bands attributed to C-H stretching modes of C_2H_6, C_3H_8 and *i*-C_4H_{10}.

Figure 4

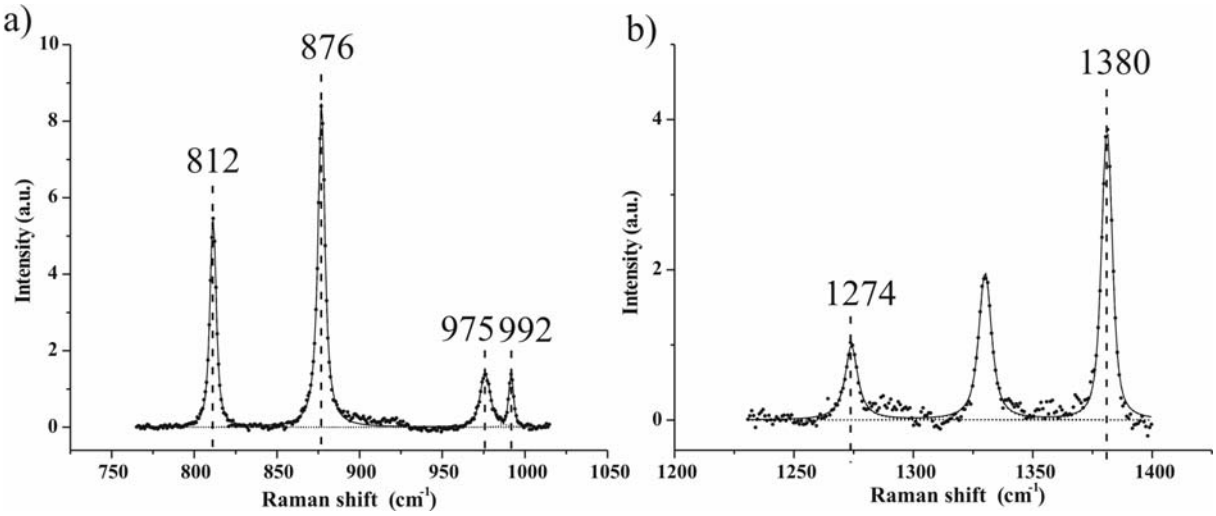

Fig. 4. a) C-C stretching spectral region of hydrocarbons (between 750 and 1050 cm^{-1}). The bands at ~812 cm^{-1}, ~876 cm^{-1} and ~992 cm^{-1} are attributed to the C-C stretching of *i*-C_4H_{10}, C_3H_8 and C_2H_6, respectively, in the large cages ($5^{12}6^4$) of type II structure. The band at ~975 cm^{-1} has not yet been assigned. b) C-O stretching spectral region (between 1250 and 1400 cm^{-1}). The bands at ~1274 cm^{-1} and ~1380 cm^{-1} can reasonably be attributed to the ν_1 (symmetric stretching C-O-C) and $2\nu_2$ (overtone of the bending mode) of the CO_2 molecules in a type II structure, whereas the band at ~1328 cm^{-1} has not yet been assigned.

Figure 5

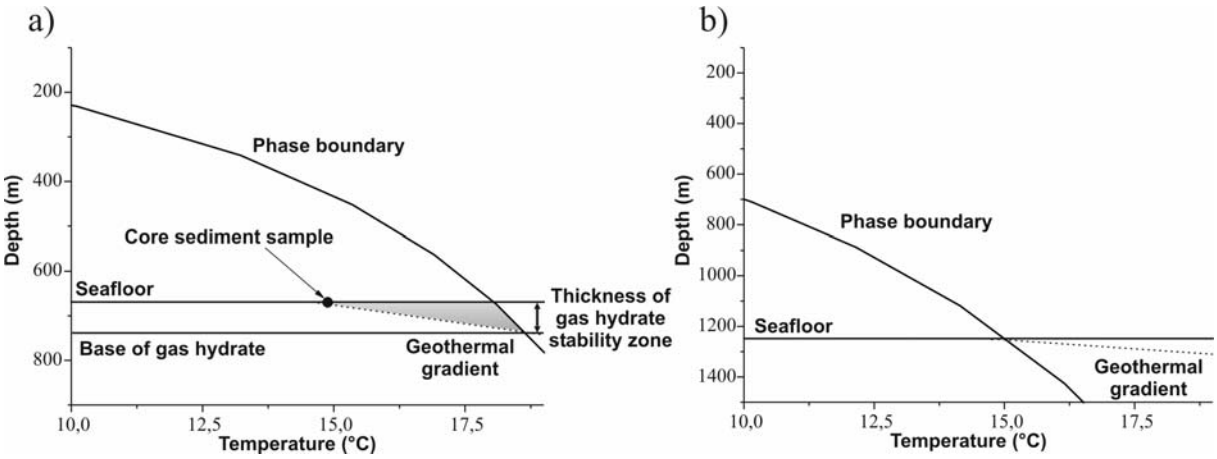

Fig. 5. Stability field of natural gas hydrate: a) deduced from gas composition of bubbles PG-1662 (Western High). The temperature and pressure conditions at the seafloor are respectively 14.5°C and 6.69 MPa. Gas hydrates are stable at such temperature and pressure conditions and the thickness of the hydrate stability zone in the sediment (shown by shaded region) can reach about one hundred meters depth, with a maximum temperature and pressure of 19°C and 7.84 MPa respectively. b) deduced from gas composition of bubbles PG-1659 (Çınarcık Basin). The temperature and pressure conditions at the seafloor are respectively 14.5°C and 12 MPa. In these conditions, which correspond to the uppermost range for gas hydrate formation, gas hydrate could form only in the first meters of sediments, but no gas hydrate associated with the PG-1659 gas bubbles have been recovered at 1200 m water depth.

Tables

Table 1. Gas and isotopic composition of gas bubbles (PG-1659, PG-1662 and PG-1664), and gas hydrate (MNTKS 27). Isotopic measurements have been performed at Isolab laboratory, the Netherlands except data in brackets obtained at TUBITAK Marmara Research Centre.

	Gas bubbles							Gas hydrate		
	PG-1659		**PG-1662**		**PG-1664**			**MNTKS 27**		
	Çinarcik Basin		***Western High***		***Central High***			***Western High***		
	Lat: 29°07.0 N		*Lat: 27°46.8 N*		*Lat: 28°35.0 N*			*Lat: 27°46.6 N*		
	Long: 40°43.0 E		*Long: 40°49.1 E*		*Long: 40°51.7 E*			*Long: 40°48.9 E*		
	Water depth: 1248 m		*Water depth: 648 m*		*Water depth: 329 m*			*Water depth: 669 m*		
Component	***Composition (%)***	***$\delta^{13}C$ (‰ PDB)***	***Composition (%)***	***$\delta^{13}C$ (‰ PDB)***	***Composition (%)***	***$\delta^{13}C$ (‰ PDB)***	***δD (‰ SMOW)***	***Composition (%)***	***$\delta^{13}C$ (‰ PDB)***	***δD (‰ SMOW)***
CH_4	99.63	–64.1	90.90	–44.4	98.86	–44.4	–210	66.10	–44.1 (–45)	–219
C_2	0.0048	–37.6	1.23	–25.7	0.48	–22.8	–119	1.23	–23.4 (–24)	–116
C_3	0.0012	–30.9	2.50	–21.1	0.24	–9.8	–132	18.8	–21.8	–151
i-C_4	0.00030	–30.2	0.93	–28	0.0039	–19.4	–132	9.50	–27.6 (–30)	–155
n-C_4	0.00030	–27.8	0.15	–20.1	0.001	–8.9	-	0.19	–22.9	-
neo-C_5	0	-	0.0034	-	0.003	–24.7	-	0.041	–25.6	-
i-C_5	0.00020	–28.3	0.31	–25.3	0.0007	–16.6	-	0.048	–25.7	-
n-C_5	0	-	0.010	–18.9	0.0003	–20.1	-	0.0002	-	-
C_6+	0.0007	-	0.0017	-	0.007	-	-	0.041	-	-
N_2	0.26	-	0	-	0.26	-	-	0	-	-
CO_2	0.10	–6.4	3.90	29.1	0.36	25.4	-	4.0	25.6	-
$C_1/(C_2+C_3)$	16600	-	24.4	-	137	-	-	3.3	-	-

Table 2: Molar composition of the hydrate and gas phases: comparison between measured concentration ($X_{i,exp}$) and modeling ($X_{i,hyd,calc}$ and $Y_{i,gas\ assoc,calc}$).

Component	$X_{i,exp}$[a]	Gas bubbles PG-1662	$X_{i,hyd,calc}$[b]	$Y_{i,gas\ assoc,calc}$[c]	*K.Marmara-af* natural gas field[d]	$X_{i,hyd,calc}$[b]	$Y_{i,gas\ assoc,calc}$[c]
CH_4	0.6610	0.9090	0.6521	0.9137	0.9100	0.6653	0.9141
C_2	0.0123	0.0123	0.0110	0.0123	0.0220	0.0181	0.0221
C_3	0.1880	0.0250	0.1823	0.0224	0.0300	0.1994	0.0272
n-C_4	0.0019	0.0015	0.0025	0.0015	0.0110	0.0150	0.0109
i-C_4	0.0950	0.0093	0.1272	0.0075	0.0080	0.0959	0.0065
n-C_5	2.0×10^{-6}	0.0001	0	0.0001	0.0040	0	0.0041
i-C_5	0.0005	0.0031	0.0004	0.0032	0.0050	0.0005	0.0051
neo-C_5	4.1×10^{-4}	3.4×10^{-5}	0	0	0	0	0
n-C_6	4.1×10^{-4}	1.7×10^{-5}	0	0	0	0	0
N_2	0	0	0	0	0	0	0
CO_2	0.0400	0.0390	0.0245	0.0393	0.0100	0.0058	0.0101

[a]$X_{i,exp}$ = experimental hydrate molar fraction of component "i"
[b]$X_{i,hyd,calc}$ = calculated hydrate molar fraction of component "i"
[c]$Y_{i,gas\ assoc,calc}$ = calculated gas molar fraction of component "i"
[d]Data from Gürgey et al. (2005)